All-reflective self-referenced spectral interferometry for single-shot measurement of few-cycle femtosecond pulses in a broadband spectral range

Zhe Si (司 哲)[1,2,†], Xiong Shen (申 雄)[2,3,†], Jingxin Zhu (朱晶鑫)[2,3], Lei Lin (林 磊)[2,3], Lihua Bai (白丽华)[1], and Jun Liu (刘 军)[2,3,*]

[1]*Department of Physics, Shanghai University, Shanghai 200444, China*

[2]*State Key Laboratory of High Field Laser Physics, Shanghai Institute of Optics and Fine Mechanics, Chinese Academy of Sciences, Shanghai 201800, China*

[3]*Center of Materials Science and Optoelectronics Engineering, University of Chinese Academy of Sciences, Beijing 100049, China*

**Corresponding author: jliu@siom.ac.cn*

Received August 26, 2019; accepted November 7, 2019; posted online December 27, 2019

An all-reflective self-referenced spectral interferometry based on the transient grating (TG) effect is proposed for single-shot measuring of the amplitude and phase of ultrashort pulses in a broadband spectral range. Except for a thin third-order nonlinear medium, which was used to generate the TG signal, no transmitted optics were used in the proposed device, and few-cycle pulses in a broad spectral range from deep UV to mid-IR can be characterized. With a homemade compact and alignment-free device, a 5.0 fs pulse at 800 nm corresponding to about two cycles and a 14.3 fs pulse at 1800 nm corresponding to less than three cycles were successfully characterized.

Keywords: transient grating; self-referenced spectral interferometry; few-cycle laser pulses; femtosecond laser pulses measurement.

doi: 10.3788/COL202018.021202.

Ultrashort laser pulses have now been widely used as important tools in many scientific research fields such as ultrahigh intense laser physics[1–3], ultrafast spectroscopy[4–6], and nonlinear optical microscopy[7]. The progress of optical metrology of ultrashort laser pulses is always tightly coupled with the development of laser sources and the extending of different applications, which always makes it a very important topic in the ultrashort laser technology field. A technique with a simple and alignment-free setup, a wide spectral application range, single-shot and few-cycle full amplitude, and phase measurement ability is required for the present advanced laser pulses and extended application.

Reliable techniques for full amplitude and phase characterization of a femtosecond pulse were consistently proposed during the last thirty years. In the late 1990s, two of the most classic methods, frequency-resolved optical gating (FROG)[8] and spectral phase interferometry for direct electric field reconstruction (SPIDER)[9], appeared, which keep optimizing since then. Several other important methods were also proposed and studied in the past decade, such as two-dimensional spectral interferometry (2DSI)[10] and multi-photon intra-pulse interference phase scan (MIIPS)[11]. However, the setup of these methods is complicated in optical setup and alignment, which limits their broad applications.

Recently, several new methods with simple and almost alignment-free setup, such as D-scan and self-referenced spectral interferometry (SRSI), have been proposed and deeply studied to fully characterize the amplitude and phase of femtosecond laser pulses. Besides the second-harmonic generation (SHG) process, several other nonlinear processes, such as self-diffraction (SD) and cross-polarized wave generation (XPW), have been studied and used in the D-scan methods recently[12–15], which allow the D-scan to be applied in a wide spectral range. SRSI is the other novel method for femtosecond pulse characterization, which was proposed in 2010. As an extension of spectral interferometry (SI)[16], SRSI is an analytical, sensitive, accurate, and fast method. The temporal profile and phase of a femtosecond pulse can be retrieved easily by the Fourier-transform SI (FTSI) algorithm[17]. In this method, a reference pulse is self-generated from the unknown pulse itself. Within a limited range of chirp, the spectrum of the reference pulse is broader than that of the unknown pulse because of the frequency-conserved third-order nonlinear process[18]. Then, we can directly obtain the spectral interferogram of the reference pulse and the time delayed unknown pulse by a spectrometer (SP). The spectral phase and amplitude of the unknown pulse can then be retrieved by FTSI.

Until now, XPW[19], SD[20], and transient grating (TG)[21] are all frequency-conserved four-wave-mixing processes that are used to generate reference pulses in the SRSI technique. Initially, the development of the SRSI method was based on the XPW process[22]. In 2011, by using LiF as a Kerr medium to generate the XPW signal, femtosecond pulses in UV were measured[23]. In the next year, 2.5 cycle pulses at 1.65 μm (13 fs FWHM) were characterized[24]. However, the use of polarizers will introduce dispersion into

 © 2019 Chinese Optics Letters

the incident pulse, thereby limiting the spectral range of the measured pulse. To solve the problem, reflective optical elements were used in XPW-SRSI to avoid the dispersion introduced by polarizers in 2015, and sub-5-fs laser pulses were measured by this optical setup[25]. The SD process was used in the SRSI method in 2012. Because of its noncollinear geometry, SD-based SRSI avoids the use of polarizers and supports wide range femtosecond pulses characterization; a 55 fs pulse at 800 nm and a sub-10-fs pulse at 400 nm were successfully characterized by this method. While the noncollinear geometry also causes troubles that the SD signal owns, angular dispersion, which may affect the measurement and the device, is relatively complicated[20]. Based on the TG effect, TG-SRSI was proposed in 2012. As TG signal generation is a self-phase-matching frequency-conserved third-order nonlinear process, TG-SRSI avoids polarizers and angular dispersion limitations in XPW-SRSI and SD-SRSI, respectively, and a 38 fs pulse at 800 nm and a sub-two-cycle 10 fs pulse at 1.75 μm were characterized. TG-SRSI also owns a higher sensitivity than the other two methods; in 2017, weak femtosecond pulses with sub-nanojoule pulse energy were successfully characterized by using an optimized TG-SRSI setup[26].

In this article, a new all-reflective TG-SRSI (AR-TG-SRSI) technique was demonstrated. A simple and almost alignment-free device was then built up with the size of about 290 mm × 170 mm × 80 mm. All metal-coated reflective mirrors and a very thin glass plate for the nonlinear process make the setup able to be run with an extremely broadband spectral range from deep UV (DUV) to mid-IR. Because there are no transmitted optical components used in this device except for the Kerr medium, and the TG process is a self-phase-matching frequency-conserved third-order nonlinear process, it can work without being bandwidth limited. At the same time, it can also be used for few-cycle femtosecond pulse characterizations due to the negligible dispersion caused by the very thin Kerr medium. To verify the ability of the method and the device, an 800 nm/5.0 fs pulse and a 1800 nm/14.3 fs pulse were characterized successfully by using the same device. This device can be used in different laser systems as a real-time monitoring device even with different center wavelengths, and it also can optimize the laser pulse output of the laser system through feedback optimization.

To achieve few-cycle pulse measurement, the transmissive polarizer is replaced by using a set of reflective polarizers in the XPW-based SRSI[25]. However, the set of reflective polarizers will limit the application spectral range of the device. Here, AR metal-coated mirrors are used, which will not only work in a broadband spectral range from DUV to mid-IR, but also with less additional dispersion in comparison to dielectric-coated mirrors. The only transmitted optic before the signal generation is a 150 μm thick fused silica glass plate, which is actually used as the nonlinear medium for TG signal generation. For the characterization of few-cycle pulses, the dispersion induced by the thin glass plate is negligible. Actually, even

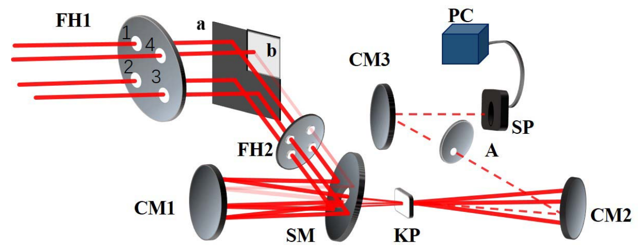

Fig. 1. Optical layout of the proposed AR-TG-SRSI. FH1 and FH2, plate with four equal-size holes; a, L-shaped metal-coated plane mirror; b, uncoated parallel mirror with fixed time-delay; SM, metal-coated mirror with a 3 mm diameter hole; CM1 and CM2, concave lens, $f = 100\,\mathrm{mm}$; KP, third-order nonlinear medium, 0.15 mm thick fused silica; A, iris; CM3, concave lens, $f = 75\,\mathrm{mm}$; SP, spectrometer.

this induced small fixed dispersion by the glass plate can be reduced in the post-process. As we all know, the TG effect in a glass plate can also work in a broadband spectral range from DUV to mid-IR. As a result, few-cycle pulses in a wide spectral range can be measured. To make a simple and almost alignment-free setup, several typical designs are involved in the AR-TG-SRSI.

Figure 1 shows the optical layout of our AR-TG-SRSI technique. A simple black plate with four equal-size holes is used to divide the input beam into four almost identical beams 1, 2, 3, and 4. The center of the four holes forms a square shape. Then, the four beams are reflected by a specially designed mirror. The mirror consists of two mirrors “a” and “b”, which are glued together. The part of “a” is an L-shaped mirror that is coated with metal film, while “b” is an uncoated mirror with a parallel and a fixed delayed surface to that of mirror “a”. This uncoated mirror b will induce a fixed time delay and is intensity-attenuated to beam 4, which is denoted as the unknown test pulse. FH2 is the second four-hole aperture and serves as a limiting hole for the light adjustment process. With the cooperation of FH1 and FH2, the direction of the incoming laser pulse can be aligned flexibly. SM is another specially designed reflective plane mirror with metal film coating. A hole is introduced in the center of the mirror SM so as to pass through the focused light of the following concave mirror CM1. All four beams are reflected onto the concave mirror CM1 and then focused onto a thin transparent plate KP through the central hole of mirror SM. As we can see, the cross-angle between the input and the output beam in CM1 is zero, which means there is no aberration in this focal process. Here, the thin plate KP is used as the third-order nonlinear medium. This vertical convergence alignment makes the four beams maintain better uniformity in the spatial structure, so that the four beams easily achieve spatial coincidence in the KP with the box coherent anti-Stokes Raman spectroscopy (BOXCARS)[27] beam geometry arrangement and generate a TG signal. On the basis of the self-phase-matching principle of the TG process, the generated TG signal is in the same direction as the unknown test pulse. CM2 is used for

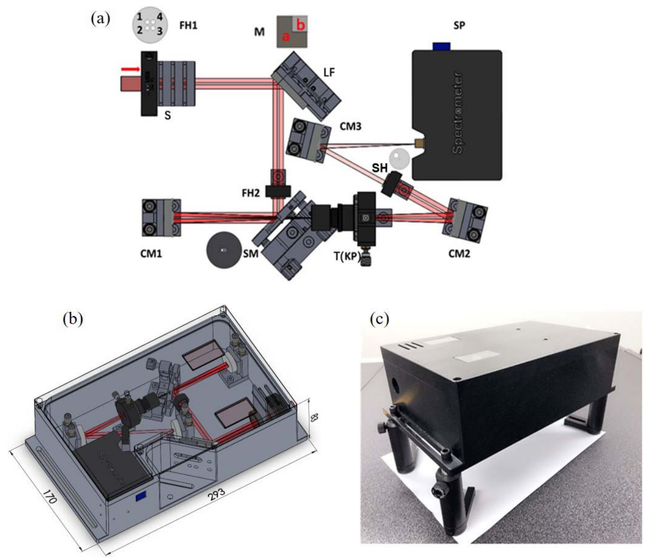

Fig. 2. (a) Sketch of the AR-TG-SRSI. (b) The schematic diagram. Size: 293 mm × 170 mm × 83 mm [their dimensions are specified in the brackets with units in millimeters (mm)]. (c) A photo of the AR device on an A4 paper.

collimating all of the beams. The combined unknown test pulse and TG signal are filtered out by using an iris A and then focused into an SP by using CM3. Since there is a suitable time delay and a proper intensity ratio between the TG signal and the unknown test pulse, a clear spectral interferogram can be obtained by the SP. Then, the temporal profile of the unknown test pulse can be retrieved by the FTSI algorithm[17].

Based on the optical layout described above, we designed a compact, robust, and alignment-free device. The schematic diagram of the device and its photo are shown in Fig. 2. As shown in Fig. 2(a), there is a 38.10 mm tube S with three narrow grooves, which also attaches FH1. Four almost identical holes are 3 mm in diameter, and the centers of the four holes form a square that has a side length of about 4.2 mm. The grooves are used for placing and fixing different light barriers so as to adjust the light path conveniently. The uncoated b region of mirror M is parallel to the front surface of the coating area a by less than 5 s and about 100 μm thinner for achieving a suitable spectral interferogram. Therefore, a simple adjustment of the energy and relative time delay of beam 4 is achieved without introducing any chirp. At the same time, the transmitted light of the b region is introduced outside the device to prevent the scattering noise caused by the reflection of other components and affect the measurement results. The third-order nonlinear medium KP (0.15 mm thick fused silica) is fixed in a 26.20 mm tube T with a certain length of screw thread, through which we can find the perfect position for the TG process around the focal point of CM1 ($f = 100\,\mathrm{mm}$). In addition, the third-order nonlinear medium KP can be moved vertically and horizontally by two knobs to avoid the defect spots due to the excessive pulse intensity around the focal spot. CM2 ($f = 100\,\mathrm{mm}$) is used for collimating all of the beams. The unknown pulse and TG signal in the direction of beam 4 can be filtered by iris A, which is then focused into the SP by CM3 with a focal length of 75 mm. The size of the device is about 290 mm × 170 mm × 80 mm, and its plane size is even smaller than the size of an A4 paper, which makes the device able to be used as a femtosecond pulse sensor or monitor inside a femtosecond laser amplifier system to improve the accuracy and efficiency of different experiments.

In this article, we first demonstrated that a device could realize single-shot characterization of few-cycle femtosecond pulses at different wavelengths. This breakthrough is owing to the AR structure of the device, which has no limit to bandwidth and introduces no dispersion. The only transmitted optical components in this device are the KP used for TG signal generation. But, we should note that only the transmitted optical components before the TG process will affect the measurement by adding fixed dispersion to incident laser pulses. To verify the ability of our new AR-TG-SRSI device, two few-cycle laser pulses at different wavelengths after a gas-filled hollow fiber for pulse compression were used to test our device. The experimental setup is shown in Fig. 3. An about 35 fs laser pulse at 800 nm, with 3 mJ energy and 1 kHz repetition rate, after a chirped-pulse-amplification Ti:sapphire laser system (Legend Elite Duo) was focused into a 3-m-long hollow fiber (with an inner diameter of 700 μm) filled with neon. A pressure gradient configuration was implemented to avoid nonlinear processes occurring before coupling the pulses into the hollow core fiber (HCF), with detrimental consequences on the performances of the compression setup in terms of coupling efficiency and carrier-envelope phase (CEP) stability. The gas pressure inside the fiber increased from < 1 mbar at the input up to 1.6 bar at the output. Pulse energy up to 2.2 mJ was obtained at the output of the chirped-mirror compressor. A pair of fused silica ultrathin wedges was placed at the input of the AR-TG-SRSI device. Taking advantage of the single-shot nature of the measurement technique, ideal dispersion compensation could be easily and rapidly obtained. To prove the measuring capability of the device in a broad spectral range, a 1800 nm femtosecond pulse

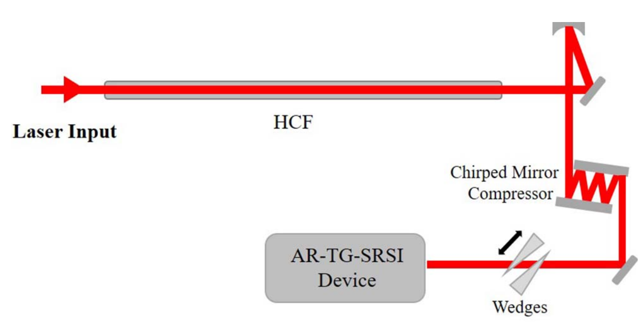

Fig. 3. Experimental setup.

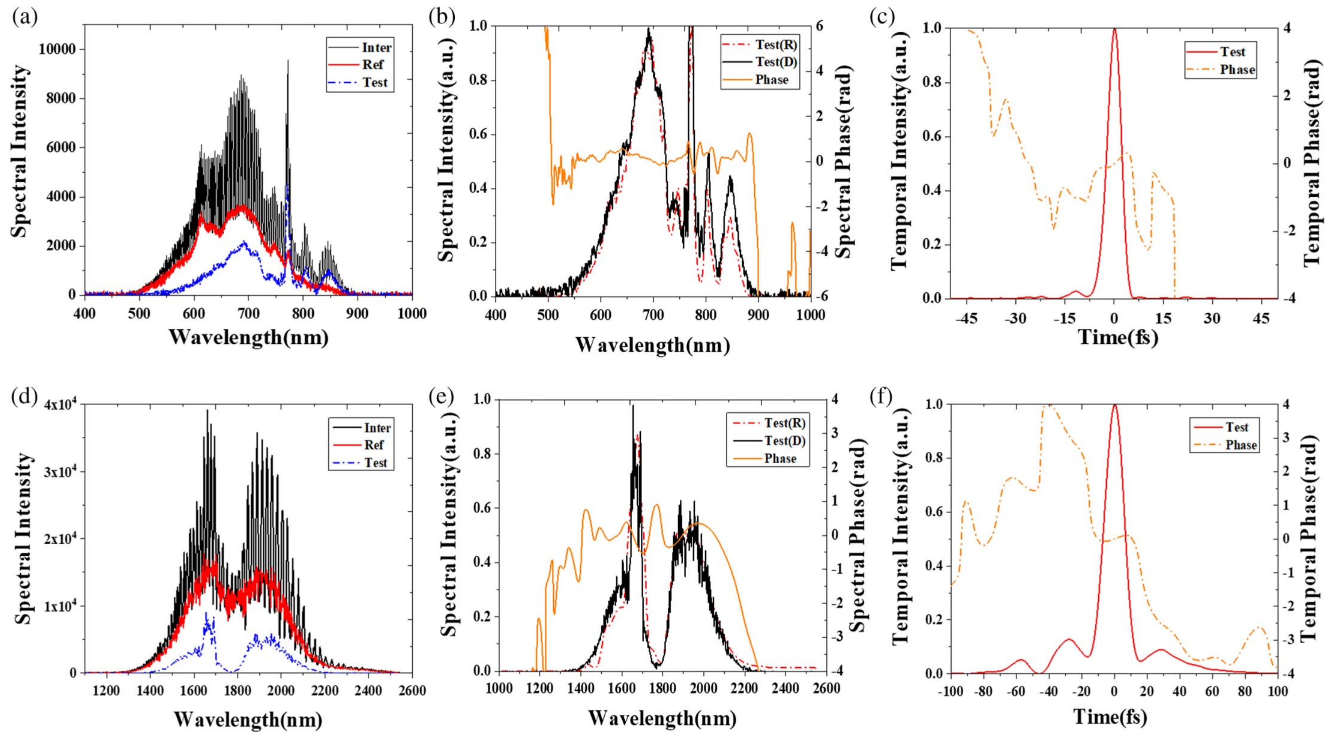

Fig. 4. (a), (d) Spectral intensity of the unknown input pulses (blue dash-dotted curve), the TG reference pulses (red solid curve), and the interference between them (black solid curve). (b), (e) Measured spectra of the unknown pulses (black solid curve), retrieved spectra of the unknown pulses (red dash-dotted curve, and retrieved spectral phases (orange solid curve). (c), (f) Retrieved temporal profile (red solid curve) and retrieved temporal phase (orange dash-dotted curve) of the unknown pulses.

from a homemade optical parametrical amplifier and a hollow fiber compressor was also measured.

Then, a 5 fs pulse at 800 nm and a 14.31 fs pulse at 1800 nm were successfully measured, respectively. The results are shown in Fig. 4. Many previous theoretical and experimental works have proved the correctness and superiority of the SRSI method[17–21]. Until now, two criteria were widely used and demonstrated to verify the fidelity of the SRSI method: one is that the spectral bandwidth of the self-created reference pulse is broader and smoother than that of the unknown input pulse, and the other is that the measured spectrum of the test pulse matches the retrieved spectrum well. The former is embodied in Figs. 4(a) and 4(d), which show the spectral intensity of the interferogram, the test pulse, and the TG signal obtained directly by SPs. The spectra of the reference pulse are smoother and broader than that of the test pulse. The latter is also embodied in Figs. 4(b) and 4(e), which show phases in the frequency domain. The retrieved spectra of unknown input pulses agree with those of the directly measured ones very well. Both results meet well with the criteria of a correct measurement using SRSI. Then, the retrieved temporal profile of unknown input pulses is obtained by the application of the FTSI algorithm. It is worth noting that we simply changed the SP from USB4000 to NIRQuest512-2.5 (Ocean Optics) to detect the spectrum at 1800 nm without changing other parts of the device.

In conclusion, a robust device for ultrashort pulse characterization based on the TG-SRSI method is proposed. Femtosecond pulses at different wavelengths were characterized by the device by simply changing different SPs. A 14.3 fs pulse at 1800 nm and a 5.0 fs pulse at 800 nm were successfully measured by this device, which speaks to the characterizing ability of the novel AR-TG-SRSI device. Furthermore, real-time monitoring of pulses can also be realized by the device, owing to the single-shot nature of the SRSI method. The optical setup is economical, alignment-free, and even smaller than the size of an A4 paper. The device can be used as a powerful instrument for femtosecond pulse monitoring in single-shot or real-time, which is very useful for a single-shot ultrahigh intense laser system and ultrahigh intense laser physics applications.

This work was supported by the Natural Science Foundation of Shanghai (No. 18ZR1413600), the National Natural Science Foundation of China (NSFC) (Nos. 61521093 and 61527821), the Instrument Developing Project of the Chinese Academy of Sciences (No. YZ201538), the Strategic Priority Research Program of the Chinese Academy of Sciences (No. XDB160106), and the Shanghai Municipal Science and Technology Major Project (No. 2017SHZDZX02).

†These authors contributed equally to this work.

References

1. F. Krausz, Rev. Mod. Phys. **81**, 163 (2009).
2. B. Shen, Z. Bu, J. Xu, T. Xu, L. Ji, R. Li, and Z. Xu, Plasma Phys. Control. Fusion **60**, 044002 (2018).

3. Z. Zhu, T. Wang, Y. Liu, N. Chen, H. Zhang, H. Sun, H. Guo, J. Zhang, X. Zhang, G. Li, and C. Liu, Chin. Opt. Lett. **16**, 073201 (2018).
4. A. H. Zewail, Angew. Chem. Int. Ed. Engl. **39**, 2586 (2000).
5. P. H. Bucksbaum, Science **317**, 766 (2007).
6. H. Guo, Z. Zhu, T. Wang, N. Chen, Y. Liu, J. Zhang, H. Sun, J. Liu, and R. Li, Chin. Opt. Lett. **16**, 033201 (2018).
7. R. G. dos Santos, L. J. Maia, C. B. de Araújo, and L. D. S. Menezes, Chin. Opt. Lett. **16**, 041902 (2018).
8. S. Adachi, N. Ishii, Y. Nomura, Y. Kobayashi, J. Itatani, T. Kanai, and S. Watanabe, Opt. Lett. **35**, 980 (2010).
9. T. Witting, F. Frank, C. A. Arrell, W. A. Okell, J. P. Marangos, and J. W. Tisch, Opt. Lett. **36**, 1680 (2011).
10. C. Manzoni, S.-W. Huang, G. Cirmi, P. Farinello, J. Moses, F. X. Kärtner, and G. Cerullo, Opt. Lett. **37**, 1880 (2012).
11. B. W. Xu, J. M. Gunn, J. M. Dela Cruz, V. V. Lozovoy, and M. J. Dantus, Opt. Soc. Am. B Opt. Phys. **23**, 750 (2006).
12. M. Miranda, T. Fordell, C. Arnold, A. L'Huillier, and H. Crespo, Opt. Express **20**, 688 (2012).
13. C. Miguel, S. Francisco, and W. Rosa, Opt. Lett. **42**, 3048 (2017).
14. A. Tajalli, B. Chanteau, M. Kretschmar, H. Kurz, D. Zuber, M. Kovačev, U. Morgner, and T. Nagy, Opt. Lett. **41**, 5246 (2016).
15. M. Louisy, C. Guo, L. Neoričić, S. Zhong, A. L'Huillier, C. L. Arnold, and M. Miranda, Appl. Opt. **56**, 9084 (2017).
16. L. Lepetit, G. Cheriaux, and M. Joffre, J. Opt. Soc. Am. B Opt. Phys. **12**, 2467 (1995).
17. T. Oksenhendler, arXiv:1204.4949 (2012).
18. M. Rhodes, G. Steinmeyer, and R. Trebino, Appl. Opt. **53**, D1 (2014).
19. T. Oksenhendler, S. Coudreau, N. Forget, V. Crozatier, S. Grabielle, R. Herzog, O. Gobert, and D. Kaplan, Appl. Phys. B Lasers Opt. **99**, 7 (2010).
20. J. Liu, Y. Jiang, T. Kobayashi, R. Li, and Z. J. Xu, Opt. Soc. Am. B Opt. Phys. **29**, 29 (2012).
21. J. Liu, F. J. Li, Y. L. Jiang, C. Li, Y. X. Leng, T. Kobayashi, R. X. Li, and Z. Z. Xu, Opt. Lett. **37**, 4829 (2012).
22. N. Minkovski, G. I. Petrov, S. M. Saltiel, O. Albert, and J. Etchepare, J. Opt. Soc. Am. B Opt. Phys. **21**, 1659 (2004).
23. S. Grabielle, S. Coudreau, V. Crozatier, N. Forget, F. Lepetit, O. Gobert, and T. Oksenhendler, in *Conference on Lasers and Electro-Optics Europe and 12th European Quantum Electronics Conference (CLEO EUROPE/EQEC)* (2011), paper CTuO3.
24. A. Trisorio, S. Grabielle, M. Divall, N. Forget, and C. P. Hauri, Opt. Lett. **37**, 2892 (2012).
25. A. Trabattoni, T. Oksenhendler, H. Jousselin, G. Tempea, S. De Silvestri, G. Sansone, F. Calegari, and M. Nisoli, Rev. Sci. Instrum. **86**, 113106 (2015).
26. X. Shen, P. Wang, J. Liu, and R. Li, Appl. Opt. **56**, 582 (2017).
27. A. C. Eckbreth, Appl. Phys. Lett. **32**, 421 (1978).